

## Variable-range hopping theory for the gap observed in strongly underdoped cuprate $\text{Bi}_2\text{Sr}_{2-x}\text{La}_x\text{CuO}_{6+\delta}$

Wei-Qiang Chen,<sup>1</sup> Jun-Qiu Zhang,<sup>1</sup> T. M. Rice,<sup>2</sup> and Fu-Chun Zhang<sup>3,4</sup>

<sup>1</sup>*Department of Physics, Southern University of Science and Technology, Shenzhen, China*

<sup>2</sup>*Institut für Theoretische Physik, ETH Zürich, CH-8093, Zürich, Switzerland*

<sup>3</sup>*Department of Physics, Zhejiang University, Hangzhou, China*

<sup>4</sup>*Collaborative Innovation Center of Advanced Microstructures, Nanjing, China*

(Received 19 March 2016; revised manuscript received 24 May 2016; published 23 June 2016)

Recent angle resolved photoemission spectroscopy experiments on strongly underdoped  $\text{Bi}_2\text{Sr}_{2-x}\text{La}_x\text{CuO}_{6+\delta}$  cuprates have reported an unusual gap in the nodal direction. Transport experiments on these cuprates observed variable-range hopping behavior. These cuprates have both electron and hole doping, which has led to proposals that this cuprate is analogous to partially compensated semiconductors. The nodal gap then corresponds to the Efros-Shklovskii (ES) gap in such semiconductors. We calculate the doping and temperature dependence of an ES gap model and find support for an Efros-Shklovskii model.

DOI: [10.1103/PhysRevB.93.241115](https://doi.org/10.1103/PhysRevB.93.241115)

The parent compound of high temperature cuprate superconductors is a Mott insulator with antiferromagnetic (AFM) long range order [1]. With doping of holes into the system, the AFM order is suppressed at first and finally vanishes at a hole concentration  $\sim 3\% - 5\%$ . When the hole concentration exceeds a critical doping  $x_c$ , the system becomes superconducting. The evolution of the system with hole concentrations is one of the central issues in the field. Many experiments have been performed in the very underdoped and low temperature regime and various phenomena have been observed, including spin glass, spin fluctuations, charge perturbations, etc. [1]. One problem is that the impurity effect in this regime is strong because of the low carrier density and high impurity concentration (each impurity introduces one hole). This has led to debates about which phenomena are intrinsic or extrinsic due to the impurities. So it is timely to investigate the impurity effects in this regime. Recently, Peng *et al.* performed angle resolved photoemission spectroscopy (ARPES) and transport experiments on a series of  $\text{Bi}_2\text{Sr}_{2-x}\text{La}_x\text{CuO}_{6+\delta}$  samples in this regime. They observed the variable-range hopping behavior in the transport experiments and an energy gap along the nodal direction in the ARPES spectra [2]. By analogy to a partially compensated semiconductor, we attribute the energy gap to the soft gap opened in the impurity band due to the Coulomb interaction between the localized electrons. This indicates that the low energy physics in this material is dominated by impurity effects. Further experimental investigations of these materials will help to separate the extrinsic phenomena originating from impurity effects from the intrinsic phenomena.

In this Rapid Communication, we examine the results of a recent series of ARPES and transport experiments on a series of  $\text{Bi}_2\text{Sr}_{2-x}\text{La}_x\text{CuO}_{6+\delta}$  samples with low hole doping, lying just below the critical doping for the onset of superconductivity. These cuprates are unusual in that large concentrations of La donors were added, which are compensated by O acceptors. A series of samples were prepared with a large La donor concentration of  $x = 0.84$ , which were annealed in an O atmosphere. The result was samples whose net carrier concentration  $P$  in the  $\text{CuO}_2$  plane is  $P < 0.10$ . Superconductivity was

observed in samples at the upper end of the doping range. Low hole doping in the planar  $\text{CuO}_2$  can only be achieved in this way, when La donors and O acceptors are arranged in tightly bound neutral states, leaving a small number of remaining holes in the more extended states in the  $\text{CuO}_2$  planes. The values of the net carrier densities that result were estimated from a series of experiments, e.g., resistivity, Hall coefficient, and thermoelectric power. This procedure led to estimates of the critical concentration for superconductivity of  $P = 0.1$ . The spatial distribution of these different states is shown schematically in Fig. 1. We will concentrate on the nonsuperconducting samples with net hole concentrations  $P < 0.1$ . We simulate the density of states with varying energy and temperature and compare with the results of the ARPES experiments.

In the ARPES experiments, one observes a peak-dip-hump structure. In the case with hole doping  $0.03 < P < 0.1$ , a gap is observed below the peak. The magnitude of the gap on the underlying Fermi surface is found to be  $k$  dependent, minimal at the nodal direction and maximal in antinodal region. The gap value is reduced with increasing hole doping and vanishes at  $P \sim 0.10$  where the system undergoes an insulator-superconductor transition. With increasing temperature, the peak becomes weaker and weaker [2]. Similar phenomena are also observed in other cuprates [3,4]. Another very important phenomenon was observed in transport experiments on samples in this doping range, namely, variable-range hopping (VRH) behavior in the resistivity [2,3]. VRH was proposed by Mott and has been well studied in semiconductors with localized impurity states forming impurity bands [5]. In partially compensated semiconductors, both acceptors and donors are present which form the acceptor bands and donor bands, respectively. In a hole doped case, the donor bands are completely empty, while the acceptor bands are partially filled. At low temperatures, the hopping of holes can only happen between acceptor states which lie very close to the chemical potential. Because the localized acceptors are randomly distributed, acceptors with a small energy difference are well separated. So the characteristic hopping length of holes will increase with decreasing temperature, leading to VRH. VRH

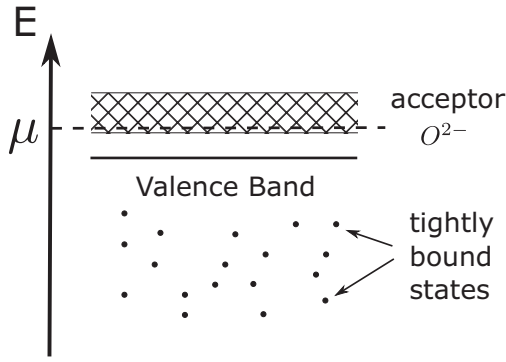


FIG. 1. A schematic figure of the band structure in lightly doped Mott insulators,  $\text{Bi}_2\text{Sr}_{2-x}\text{La}_x\text{CuO}_{6+\delta}$  with both hole and electron dopants, similar to partially compensated semiconductors. The upper Hubbard band (not shown) acts as a conduction band, and the valence band is the lower Hubbard (or Zhang-Rice) singlet band.  $\text{La}^{3+}$  impurities form a donor band below the bottom of the conduction band, and the compensating  $\text{O}^{2-}$  ions form an acceptor band above the top of the valence band. Some holes and electrons form local bound states due to the strong attraction between the nearby  $\text{La}^{3+}$  and extra  $\text{O}^{2-}$  ions, with energies well below the top of the valence band. The chemical potential lies within the acceptor band due to the excess of holes.

makes the system an insulator although the acceptor band is only partially filled, leading to a resistivity which varies as  $\rho_0 \exp[(T_0/T)^\alpha]$  with temperature. The exponent  $\alpha$  is 1/3 in two dimensions (2D) if there is a finite density of states (DOS) at the Fermi level [5]. But Efros and Shklovskii (ES) pointed out later that because of the long range Coulomb interaction between the localized charges, a soft gap will open at the chemical potential at zero temperature [6]. The direct consequence of the opening of the ES gap is that the exponent becomes  $\alpha = 1/2$  at very low temperatures. With increasing temperature, the ES gap is filled and the exponent  $\alpha$  will be reduced to 1/3.

In the experiments on  $\text{Bi}_2\text{Sr}_{2-x}\text{La}_x\text{CuO}_{6+\delta}$ , the transport data were fitted with the VRH form for both  $\alpha = 1/3$  and 1/2. But the fitting to an exponent 1/2 is only good at low temperatures, while the fitting to 1/3 is good at a much larger temperature region [7]. On one hand, this indicates a VRH physics in the  $\text{Bi}_2\text{Sr}_{2-x}\text{La}_x\text{CuO}_{6+\delta}$  system. On the other hand, the exponents indicate a gap opens at low temperature which fills up as the temperature is raised. Similar with the partially compensated semiconductor, the  $\text{Bi}_2\text{Sr}_{2-x}\text{La}_x\text{CuO}_{6+\delta}$  material also has two kinds of dopants, the  $\text{La}^{3+}$  and the extra  $\text{O}^{2-}$ , which introduce the electrons and holes, respectively. So it is natural to make an analogy between the  $\text{Bi}_2\text{Sr}_{2-x}\text{La}_x\text{CuO}_{6+\delta}$  and partially compensated semiconductors, where the  $\text{La}^{3+}$  and extra  $\text{O}^{2-}$  play the roles of donors and acceptors, respectively.

As discussed above, the VRH behavior in  $\text{Bi}_2\text{Sr}_{2-x}\text{La}_x\text{CuO}_{6+\delta}$  material at low temperatures indicates the opening of an ES gap. This gap should correspond to the gap observed in the experiments [2,3]. To investigate the properties of the ES gap, we follow earlier calculations [6,8–10] and

study the following classical Hamiltonian,

$$H = \sum_i n_i \phi_i + \frac{V}{2} \sum_{i \neq j} \frac{n_i n_j}{r_{ij}}, \quad (1)$$

where  $i$  is the index of the center of an impurity in the acceptor bands,  $\phi_i$  is the energy of the corresponding localized state,  $n_i = 0, 1$  is the occupation number of holes in the state,  $V = e^2/4\pi\epsilon_r\epsilon_0 a$  is the coupling strength of the Coulomb repulsion between two holes,  $\epsilon_r$  is the dielectric constant, and  $r_{ij}$  is the distance between two impurities  $i$  and  $j$ . Note, this classical Hamiltonian ignores possible precursor hole pairing effects as the superconducting state is approached, e.g., as proposed in a recent paper by Mueller and Shklovskii [11]. In our calculation, for simplicity, we assume that the impurities form a square lattice. This approximation should not affect the result because only the states around the chemical potential are important, and those states are spatially separated and have randomly distributed energies, as pointed out in Ref. [9]. As mentioned above, most O acceptors form tightly bound neutral states with La donors and only a small fraction of extra  $\text{O}^{2-}$  show up in the acceptor band, i.e., the effective concentration  $n_a$  of O acceptors per Cu site is much smaller than the nominal one,  $\delta = (x + P)/2 = 0.42 + P/2$ . This leads to the uncertainty to estimate the charge carrier's filling  $\nu_h$  in the acceptor band, which is defined by

$$\nu_h = P/n_a, \quad (2)$$

with  $P$  the concentration of doped holes in a Cu-oxide plane. Since  $n_a < \delta$ , we have  $\nu_h > P/\delta$ . While the precise relation between  $n_a$  and  $\delta$ , hence the relation between  $\nu_h$  and  $P$ , depends on the specific material, it is reasonable to assume  $\nu_h$  and  $P$  are monotonic: A larger value of  $\nu_h$  corresponds to a larger  $P$  in ARPES. In the calculations below, we consider three different values of  $\nu_h$ : 0.88, 0.92, and 0.96. We restrict our calculations to the DOS relevant for ARPES experiments. Note, simulations for the VRH conductivity in a similar model were carried out by Levin *et al.* [10].

First, we consider the density of states at zero temperature of a  $10 \times 10$  lattice with periodic boundary conditions. The DOS are calculated and averaged over  $10^6$  impurity configurations. In the calculations, the bandwidth of the acceptor band is chosen to be 200 meV, i.e.,  $\phi_i$  is generated randomly in the interval  $[-100, 100]$  meV. The Coulomb coupling strength  $V$  is chosen to be 100 meV, which corresponds to  $\epsilon_r \approx 38$ . The electron distribution with lowest energy for each configuration is achieved with the procedure used in Refs. [8,9]. At first, we generate an initial distribution of the holes randomly for a given impurity configuration. Then we apply the so-called  $\mu$ -sub procedure. We calculated the single particle energy for each state with

$$E_i = \phi_i + \sum_{j \neq i} \frac{n_j}{r_{ij}}, \quad (3)$$

where  $r_{ij}$  is the shortest distance between two sites  $i$  and  $j$ . If  $E_i$  of the highest occupied site is larger than  $E_i$  of the lowest empty site, we will move the hole from the highest occupied site to the lowest empty site. Then we recalculate  $E_i$  and do the check again and again until all  $E_i$  of the occupied sites are less than any  $E_i$  of the empty sites.

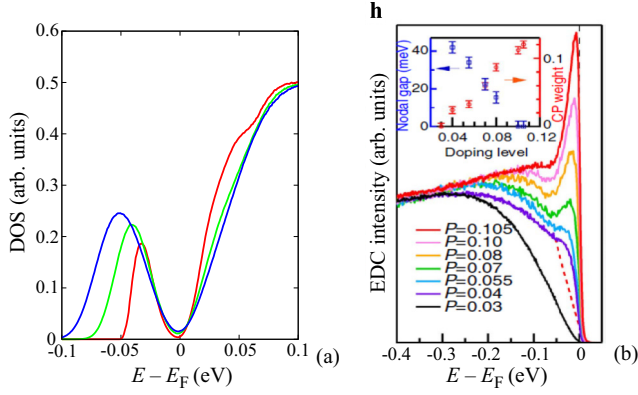


FIG. 2. (a) Calculated electron density of states (DOS) for various of filling factors of holes,  $\nu_h$  in the impurity acceptor band:  $\nu_h = 0.88$  (blue line),  $\nu_h = 0.92$  (green lines), and  $\nu_h = 0.94$  (red lines), respectively. (b) The ARPES data on the energy distribution curve (EDC) for various hole dopings  $p$ , from Fig. 3 in Ref. [2]. The right panel in (b) shows only the occupied electron states which are observed in ARPES. Note that the position of the DOS peak shown in (a) shifts towards zero as  $\nu_h$  increases, qualitatively consistent with the ARPES data, showing the peak position in EDC shifts towards zero as  $p$  hence  $\nu_h$  increases.

In the next stage, we check the energy for a single hole, which hops with

$$E_{ji} = E_j - E_i - \frac{1}{r_{ij}}, \quad (4)$$

where  $i$  is an occupied site and  $j$  is an empty site. The hop will be performed if  $E_{ji} < 0$ . After each hop, we redo the  $\mu$ -sub process and check all possible single hole hops until all  $E_{ji}$  are positive. Then we take the resulting hole distribution as one candidate ground state. After 5000 iterations of the whole process for a given impurity configuration, we choose the one with lowest energy from all the candidates and choose it as the ground state for that impurity configuration.

With the single particle energy of the ground states, we can get the DOS by averaging over all the impurity configurations: The result is shown in Fig. 2(a), where the DOS at  $\nu_h = 0.88$  (blue line), 0.92 (green line), and 0.96 (red line) are depicted. To compare with the ARPES experiment, the DOS is presented in electron notation. It is obvious that a soft gap opened at the chemical potential for all three cases at low temperatures. The finite DOS at the chemical potential at the larger hole doping case may due to the finite size effect. The most important feature is that the peak position is shifted towards zero as the hole doping  $p$  increases, which is qualitatively consistent with the experimental result shown in Fig. 2(b), which is extracted from Fig. 3 in Ref. [2].

Then we study the DOS at finite temperature with the Monte Carlo technique used in Ref. [9]. At first, we generate  $10^4$  random configurations of  $\phi$ . For each configuration, we calculate the single particle energies from higher temperature to lower temperature with a standard Monte Carlo algorithm. At each temperature, we drop the first  $10^4$  hole configurations to remove the memory of higher temperature and keep the single particle energies for the next  $10^5$  hole configurations. By averaging over all the impurity configu-

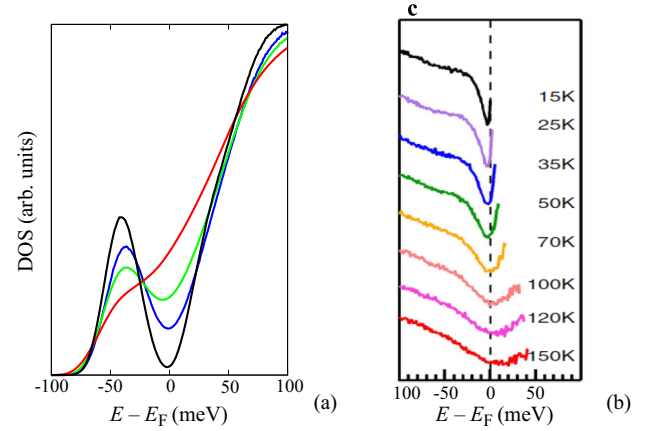


FIG. 3. (a) Calculated DOS at impurity acceptor band filling factor  $\nu_h = 0.92$  at various temperatures:  $k_B T = 0$  (black line), 6 meV (blue line), 10 meV (green line), and 20 meV (red line), respectively. (b) The ARPES result for the energy distribution curve (after dividing the Fermi function) at various temperatures, extracted from Fig. 4 in Ref. [2]. See the text for a discussion of the qualitative agreement between the theory and experiment.

rations, we get the DOS at finite temperature. The result for  $\nu_h = 0.92$  at temperatures  $k_B T = 0$  (black line), 6 meV (red line), 10 meV (green line), and 20 meV (blue line) are depicted in Fig. 3(a). With increasing temperature, the amplitude of the peak decreases while the DOS at the chemical potential increases, leading to the closing of the ES gap. Note the positions of the peaks shift only slightly to lower energy with increasing temperature. These results are consistent with the experiment shown in Fig. 3(b), which is extracted from Fig. 4 in Ref. [2].

Another feature of the ARPES experiments is the momentum dependence of the ES gap which is minimal at the nodal point and increases away from the nodal point. This momentum dependence may originate from the spatial distribution of the impurities which could be affected by various effects such as clustering, etc., at such high impurity densities. But, in our model, we only consider the random distributed impurities because of the lack of information on the actual spatial distribution.

We have carried out simulations of the electron density of states for lightly doped cuprates with strong random potentials and compensated electron and hole dopings, and compared them to the results of ARPES experiments on nonsuperconducting  $\text{Bi}_2\text{Sr}_{2-x}\text{La}_x\text{CuO}_{6+\delta}$  samples whose transport properties show variable-range hopping at low temperatures. The ARPES experiments measure only states occupied by electrons with energies strictly below the chemical potential at low temperatures, extending to slightly above as  $T$  is raised. Our simulations show good agreement with the key features in the density and temperature dependence of the electron density of states, and support the interpretation put forward by Zhou and collaborators of their experimental results.

We thank X. J. Zhou for interesting discussions and allowing us to reuse the figures in their paper. W.Q.C. is partly supported by NSFC 11374135, and F.C.Z. thanks NSFC 11274269, and National Basic Research Program of China (No. 2014CB921203).

- [1] B. Keimer, S. A. Kivelson, M. R. Norman, S. Uchida, and J. Zaanen, *Nature (London)* **518**, 179 (2015).
- [2] Y. Peng, J. Meng, D. Mou, J. He, L. Zhao, Y. Wu, G. Liu, X. Dong, S. He, J. Zhang, X. Wang, Q. Peng, Z. Wang, S. Zhang, F. Yang, C. Chen, Z. Xu, T. K. Lee, and X. J. Zhou, *Nat. Commun.* **4**, 2459 (2013).
- [3] Z.-H. Pan, P. Richard, Y.-M. Xu, M. Neupane, P. Bishay, A. V. Fedorov, H. Luo, L. Fang, H.-H. Wen, Z. Wang, and H. Ding, *Phys. Rev. B* **79**, 092507 (2009).
- [4] K. M. Shen, T. Yoshida, D. H. Lu, F. Ronning, N. P. Armitage, W. S. Lee, X. J. Zhou, A. Damascelli, D. L. Feng, N. J. C. Ingle, H. Eisaki, Y. Kohsaka, H. Takagi, T. Kakeshita, S. Uchida, P. K. Mang, M. Greven, Y. Onose, Y. Taguchi, Y. Tokura, S. Komiyama, Y. Ando, M. Azuma, M. Takano, A. Fujimori, and Z.-X. Shen, *Phys. Rev. B* **69**, 054503 (2004).
- [5] N. F. Mott, *J. Non-Cryst. Solids* **1**, 1 (1968).
- [6] A. L. Efros and B. I. Shklovskii, *J. Phys. C* **8**, L49 (1975); B. I. Shklovskii and A. L. Efros, *Fiz. Tekh. Poluprovodn.* **14**, 825 (1980) [*Sov. Phys. Semicond.* **14**, 487 (1980)].
- [7] X. J. Zhou (private communication).
- [8] S. D. Baranovskii, A. L. Efros, B. I. Gelmont, and B. I. Shklovskii, *J. Phys. C* **12**, 1023 (1979).
- [9] J. H. Davies, P. A. Lee, and T. M. Rice, *Phys. Rev. B* **29**, 4260 (1984).
- [10] E. I. Levin, V.L. Nguen, B. I. Shklovskii, and A. L. Efros, *Zh. Eksp. Teor. Fiz.* **84**, 1499 (1987).
- [11] M. Mueller and B. I. Shklovskii, *Phys. Rev. B.* **79**, 134504 (2009).